Supplementary section:

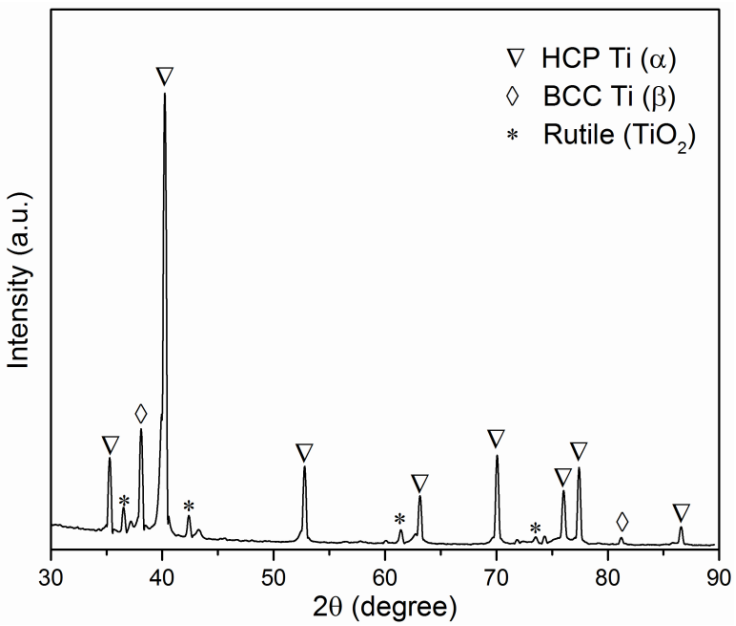

Fig. S1: X-ray diffraction pattern of sintered Ti-6Al-4V showing the predominance of the HCP α-phase in the microstructure. Some extent of rutile formation was also evident which was probably due to exposure of the powder in the air during printing and utilization of the aqueous binder.

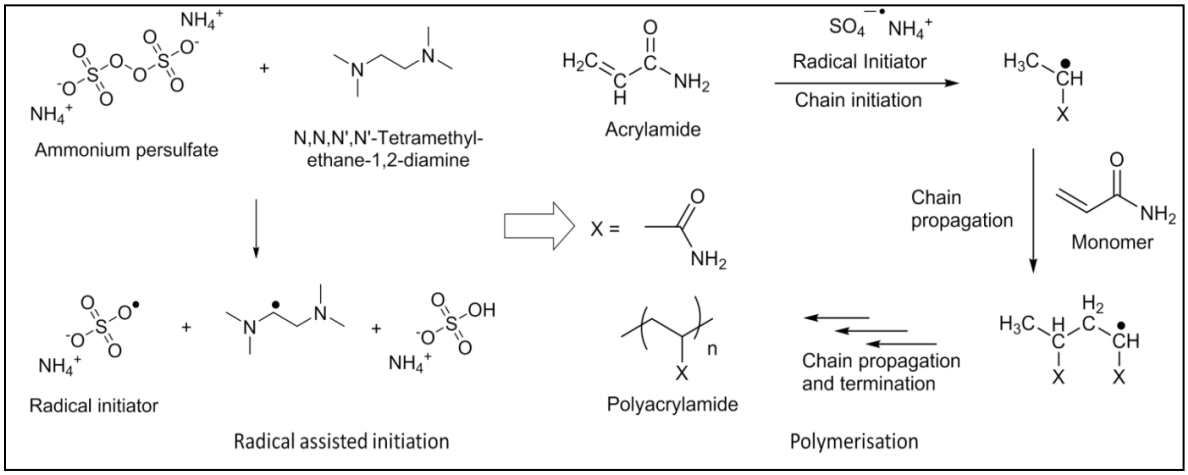

Fig. S2: *in situ* polymerization plays the key role in powder-ink interaction. Schematic of the adapted polymerisation reaction of acrylamide added with TEMED in the presence of APS pre-mixed with the powder to be printed. TEMED stabilizes the nascent free radicals generated from the dissociation of persulfate bond of APS and assists to attack the α-center of acrylamide. The reactive free radical site of the monomer attacks double bonds of other monomers present in the solution and add them subsequently to the backbone to increase the chain length.

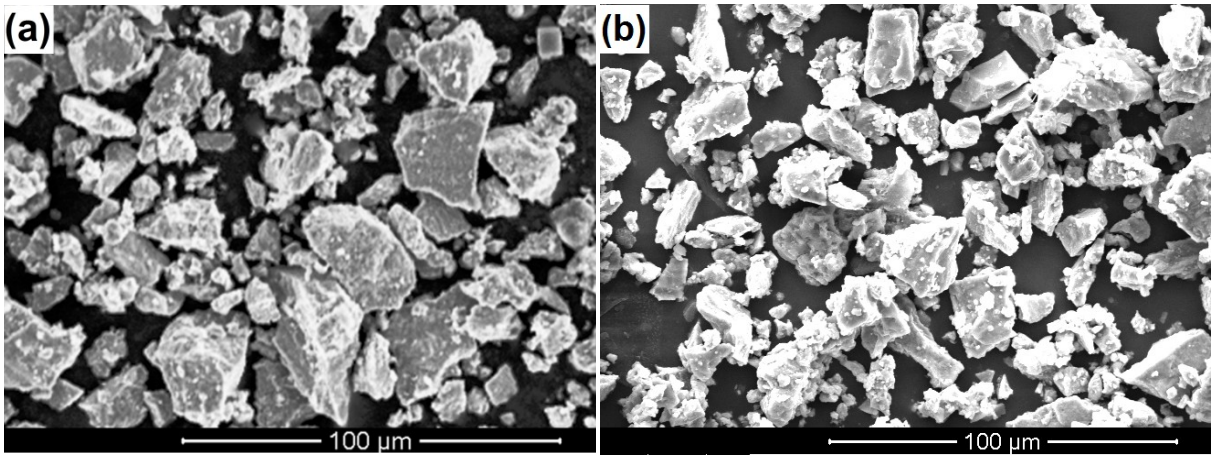

Fig. S3: Powder particle diameter influences the ink infiltration time. Morphology of the as received (a) and APS modified Ti-6Al-4V powders by ball milling (b).

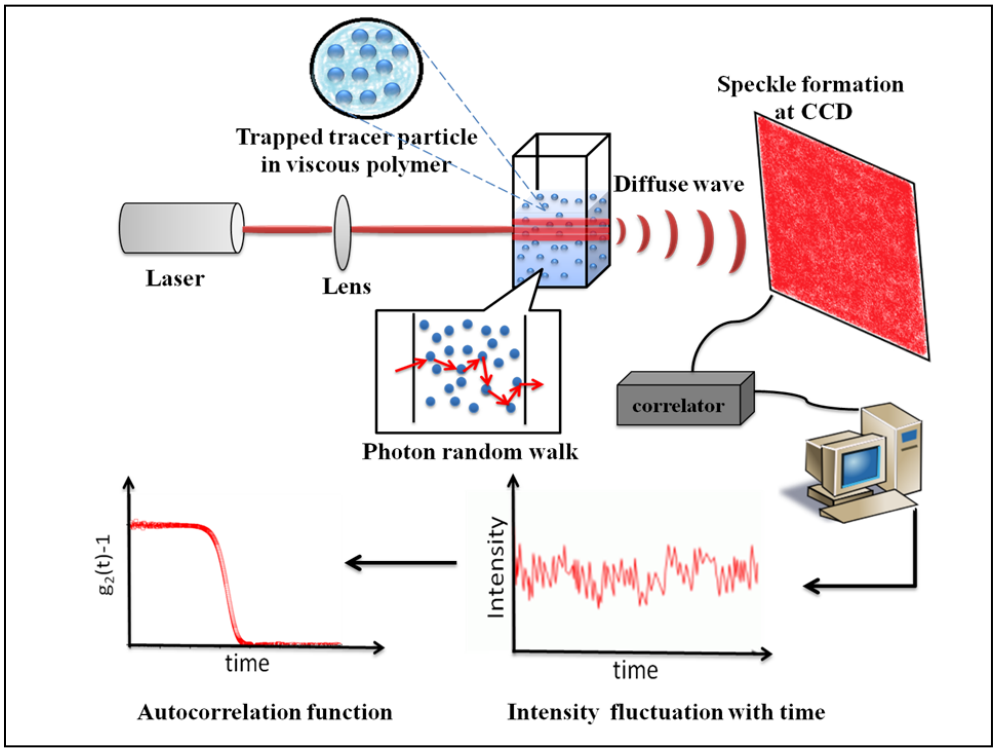

Fig. S4: Schematic representation of working principle of diffusing wave spectroscopy. The delayed decay in autocorrelation function attributes to the more intermediate interactions with the macromolecules interfering in the optical path.

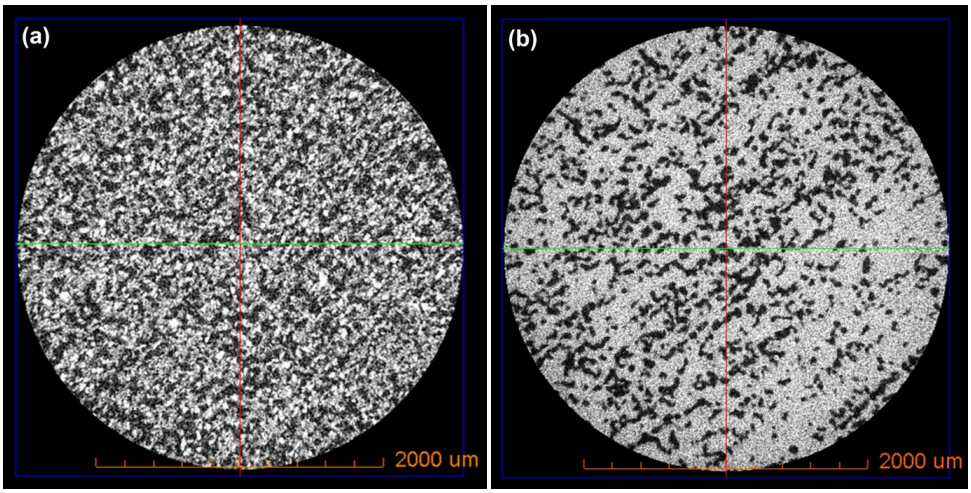

Fig. S5: 2D porous surface morphologies perceived from the orthoslices of as-printed Ti-6Al-4V (a) and as-sintered Ti-6Al-4V (b), obtained from high resolution micro-CT scan. The decrease in pore number, interconnectivity and increment in pore sizes are clearly visible after sintering.

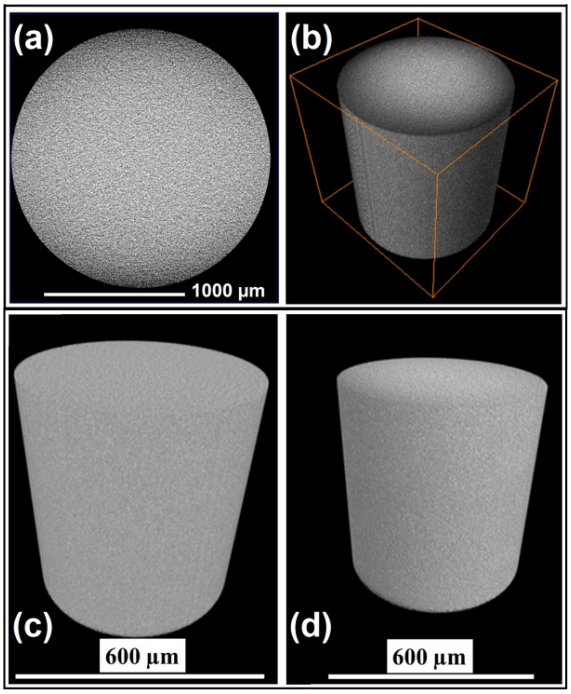

Fig. S6: The 2D orthoslice (a) and 3D volume rendered microstructure (b) from micro-computed tomogram of the non-porous metallurgically processed (commercial) Ti-6Al-4V. 3D volume rendered non-porous microstructure of the SLM Ti-6Al-4V referred in this study[38] (permission granted by Elsevier for reproducing in this article); (c) horizontally printed and (d) vertically printed samples

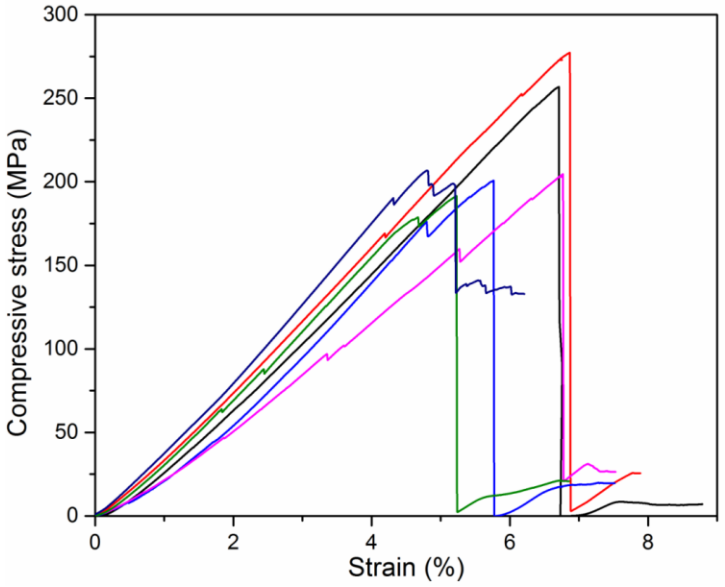

Fig. S7: Representative stress-strain plots of printed-sintered microporous Ti-6Al-4V cylinders demonstrate brittle nature of failure. The kinks appear due to progressive failure of the porous layers.

- **Fibronectin assay for immunocytochemistry of 3T3 cells**

3T3 cells grown on the surfaces of inkjet printed microporous Ti-6Al-4V and commercially available Ti-6Al-4V along with the controls were fixed by using 4% paraformaldehyde (PFA, SDFCL) solution. Subsequently, the cells were permeabilised with 0.1% of triton X and blocked with 1% Bovine Serum Albumin (BSA) to prevent the unwanted non-specific binding of the dye. Primary antibodies of fibronectin (Abcam, ab2413) were added at dilution of 1:200 for 1 h. Secondary antibody of goat with fluorophore tagging [AF488 (A 11029)] was added at the 1:650 dilution and kept for 1 hr. The cells were observed under fluorescence microscope (Nikon LV 100D, Japan).

The modulated cytocompatibility of the 3D printed Ti-6Al-4V corroborates well with the fibronectin protein expression. The extent of focal adhesion complexes on a biomaterial substrate, in turn, mediates the cell attachment, and further triggers cell spreading and proliferation. From **Fig. S8,** it is observed that, the expression of the interactive fibronectin

proteins (green spots in group) are higher in the case of 3D inkjet printed Ti-6Al-4V, when compared to control and the commercial Ti-6Al-4V.

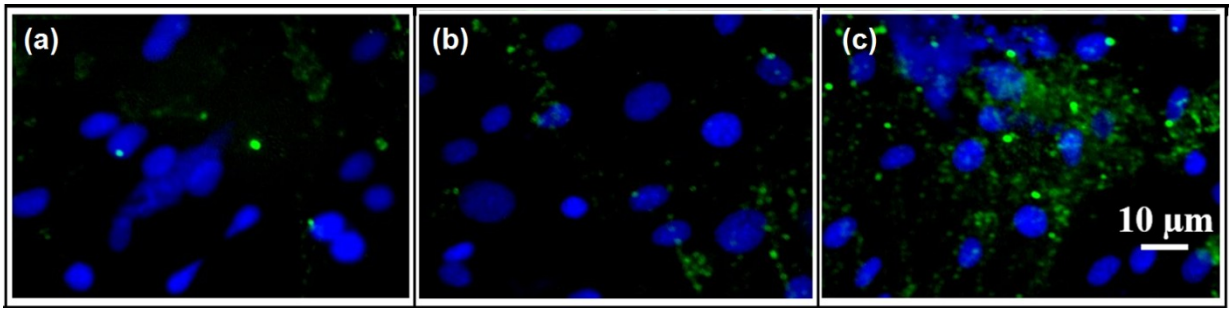

Fig. S8: Enhanced fibroblast adhesion was evidenced in the fibronectin protein expression, where extensive focal adhesion complex linking the integrin proteins was found to be present on inkjet printed Ti-6Al-4V (c), indicating good cell-material adhesion. The green spots essentially express the fibronectin protein around cell-biomaterial interface. The fluorescent green spots in (a) and (b) represent the fibronectin expression of TCPS control and commercial Ti-6Al-4V respectively.

- **Calcium activity of 3T3 cells on commercial and 3DIJPP Ti-6Al-4V**

Fluo-4 AM is a non-toxic calcium detecting fluorescent probe. The loading of the dye to live cells is essential for detecting calcium activities, which indicate both survivability and apoptosis, depending on the ion concentration. The cultured fibroblasts were loaded with Fluo-4 AM (Invitrogen) using the final concentration of 2 µM along with 0.1% Pluronic F-127 in 1 mL of HEPES buffer. The later was used as the loading detergent. The samples were incubated at 37 °C for 30 min and the dye was allowed to be deesterified by the cellular activities which enhance the intensity of the emitted fluorescence. The dye loaded cells with tagged intracellular-calcium were imaged in a fluorescence microscope using excitation wavelength of 494 nm and emission at 516 nm. Calcium (Ca^{2+}) ions take part in cellular signaling in terms of triggering various allosteric regulatory influences on various enzymes and proteins. As shown in **Fig. S9**, the

calcium activities after 6 days of culture for the fibroblasts on the 3D inkjet printed Ti-6Al-4V specimens exhibited almost similar behavior like the TCPS control and commercial Ti-6Al-4V. This is also consistent with the Ca-intensity plots, measured on the basis of fluorescence intensity variation.

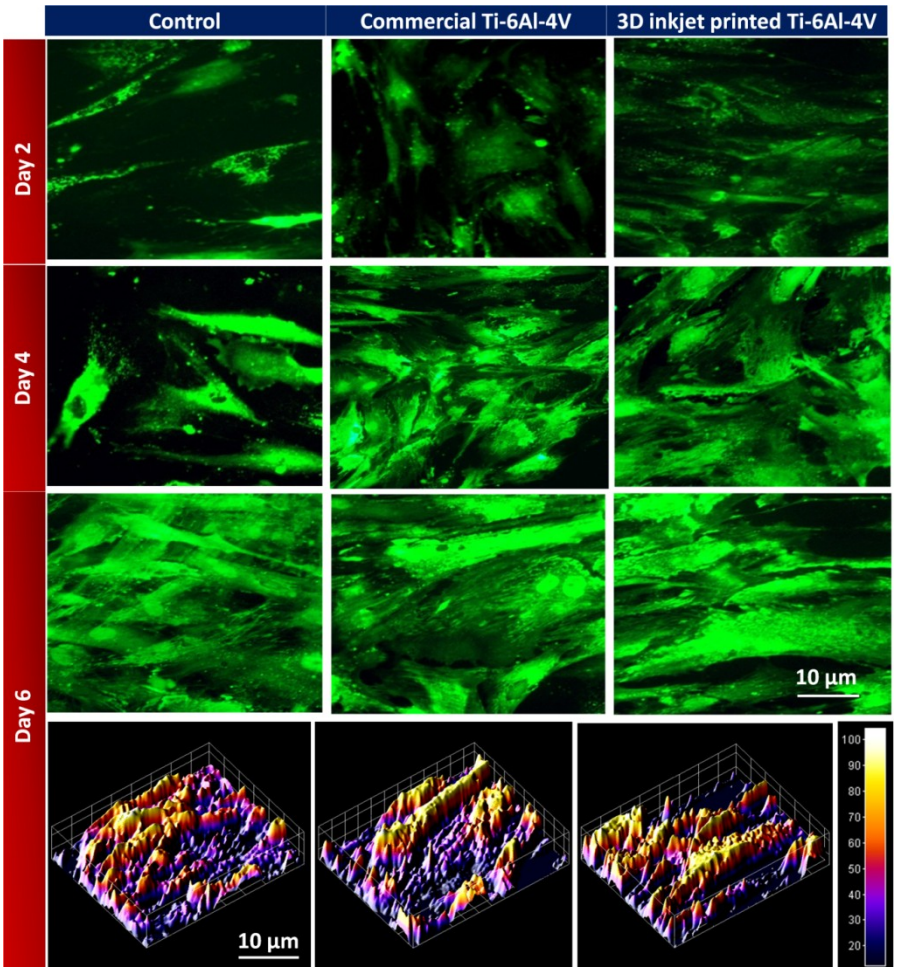

Fig. S9: Fluo-4 AM staining of cultured cells provide signatures of intracellular calcium activity. Representative fluorescence microscopic images of Fluo-4 tagged 3T3 murine fibroblasts on the 3D inkjet printed Ti-6Al-4V and the commercial Ti-6Al-4V at different time points in culture, exhibiting metabolically healthy cellular activities. The dynamic increments in the Ca2+ expressions are similar on all the biomaterial substrates. The color scale depicts the entire range of the Ca2+ expression, evolving from the blue (zero expression) towards white (maximum expression).